

The rotation measures of high luminosity sources as seen from the NVSS.

M. S. Pshirkov^{1,2,3*}, P. G. Tinyakov^{3,4†}, F. R. Urban^{4‡}

¹*Sternberg Astronomical Institute, Lomonosov Moscow State University, Universitetsky prospekt 13, 119992, Moscow, Russia*

²*Pushchino Radio Astronomy Observatory, 142290 Pushchino, Russia*

³*Institute for Nuclear Research of the Russian Academy of Sciences, 117312, Moscow, Russia*

⁴*Université Libre de Bruxelles, Service de Physique Théorique, CP225, 1050, Brussels, Belgium*

ABSTRACT

We re-analyse the subset of the Faraday rotation measures data from the NRAO VLA Sky Survey catalogue for which redshift and spectral index information is available, in order to better elucidate the relations between these observables. We split this subset in two based on their radio luminosity, and find that higher power sources have a systematically higher residual rotation measure, once the regular field of the Milky Way is subtracted. This rotation measure stands well above the variances due to the turbulent field of our Galaxy and measurement errors, contrarily to low power sources. The effect is more pronounced as the energy threshold becomes more restrictive. If the two sets are merged one observes an apparent evolution of rotation measure with redshift, but our analysis shows that this can be interpreted as an artifact of the different intrinsic properties of brighter sources that are typically observed at larger distances.

Key words: IGM: magnetic fields

1 INTRODUCTION

Magnetic fields (MFs) seem to be omnipresent in the Universe, from the Earth to the huge intergalactic voids (Kronberg 1994; Han & Wielebinski 2002; Govoni & Feretti 2004; Vallée 2004; Ryu et al. 2012), including stars, galaxies, clusters, and perhaps filaments. They were observed in galaxies at high redshift $z > 1$ when the Universe was only a few billions years old (Kronberg et al. 2008; Bernet et al. 2008).

MFs also permeate the Large Scale Structure (LSS) of the Universe: it is typically believed that they were initially created in the astrophysical sources within the LSS, and only afterwards they polluted the LSS itself. The MFs that are tentatively observed in the voids (Neronov & Vovk 2010; Tavecchio et al. 2010; Dolag et al. 2011; Taylor et al. 2011)¹ could also be blown away from the LSS; alternatively, they could be of primordial origin—cosmological inflation, early universe phase transitions, etc (Grasso & Rubinstein 2001; Dolgov 2003; Kandus et al. 2011; Durrer & Neronov 2013).

Since there are no compelling models for their genesis, it is crucial to better understand their morphology, strength, spectral properties, and distribution in the Universe; the more so for extragalactic fields, for which the very large correlation lengths are theoretically difficult to achieve.

One of the most effective ways to study such extragalactic MFs is through the observations of Faraday rotation measures (RMs). The plane of polarization of a linearly polarized electromagnetic wave of wavelength λ travels through a magnetized plasma rotates by the angle $\Delta\psi$ proportional to the square of the wavelength,

$$\Delta\psi = \text{RM} \cdot \lambda^2. \quad (1)$$

Thus one needs multi- or at least bi-frequency observations in order to determine the rotation measure RM. The value of RM depends on the properties of the medium and the permeating magnetic field as follows,

$$\text{RM} = 812 \int_D n_e B_{||} dl, \quad (2)$$

where n_e is the density of free electrons measured in cm^{-3} , $B_{||}$ is the component of the magnetic field parallel to the line-of-sight measured in μG (positive when directed towards the observer), and D is the distance from the observer to the source in kpc. Hence, an independent estimate of the electron density n_e is required to deduce information on the magnetic field proper from Faraday rotation measures.

* E-mail: pshirkov@sai.msu.ru

† E-mail: petr.tiniakov@ulb.ac.be

‡ E-mail: furban@ulb.ac.be

¹ This is however by no means a settled issue, see (Broderick et al. 2012; Murase et al. 2012; Miniati & Elyiv 2013; Beck et al. 2013; Neronov et al. 2013; Saveliev et al. 2013; Sironi & Giannios 2014)

An indirect evidence of the MF presence in LSS and in voids may be obtained by studying the redshift evolution of RM of an ensemble of extragalactic sources. In a recent paper (Neronov et al. 2013) some evidence for a significant redshift evolution in the RMs from the catalogue (Hammond et al. 2012) was reported: the RMs were found to be growing with redshift in a way that could be interpreted as a sign of non-zero nanoGauss-scale MFs in the filaments of the LSS. Such redshift dependence was not observed in the original catalogue (Hammond et al. 2012); moreover, a recent work (Banfield et al. 2014) while re-examining the same dataset (although retaining a smaller portion of it), did not find indication for a very significant systematic correlation with redshift. Finally, most recently another analysis (Xu & Han 2014) reported on a quite weak evolution with redshift, again for a very similar set.

We assess these claims in what follows, where in addition to previous analyses we also search for a possible systematic dependence of the measured RMs on intrinsic properties of sources, in particular their radio luminosity. We perform several tests, from which a coherent interpretation emerges:

- we found no indication of a redshift evolution caused by the intervening medium;
- we do observe a sort of Malmquist bias, i.e., in a flux-limited sample we detect sources with higher luminosities at larger distances—the further we go, the higher the mean luminosity, thus mimicking an apparent redshift evolution by the redshift-dependent selection of sources with intrinsically different properties;
- the residual RM in low luminosity sources appears to be mostly due to the turbulent random Galactic MF (rGMF) and measurement errors, and consequently does not change with redshift;
- the residual RM in high luminosity sources instead shows a *systematic* bias above the contribution from rGMF plus measurement errors; however, there is also no clear redshift evolution in this set;
- this bias grows with more selective luminosity cutoffs, that is, there appears to be a positive correlation between the residual RM and the radio luminosity of the source.

The rest of this paper is organised as follows. First, in Sec. 2 we introduce the data and our selection, cleaning, and averaging procedures. Sec. 3 reports all of our results and their interpretation. Finally, we summarise our findings in Sec. 4.

2 DATA AND METHODS

The data. The largest set of RMs of extragalactic sources to date was compiled in (Taylor et al. 2009) from re-analyzing the NRAO VLA Sky Survey (NVSS) data. The NVSS is the largest by number survey of polarized radio sources at declinations $> -40^\circ$ (Condon et al. 1998). The survey was performed in two nearby bands, 1364.9 and 1435.1 MHz; each having a width of 42 MHz. Observations at these close frequencies then give estimations of the RMs of the sources. The total number of observed sources was 37,543. More than 10% of these sources have redshifts assigned (Hammond et al. 2012).

We selected 4002 NVSS sources with known redshifts from (Hammond et al. 2012). Also we imposed the following cuts: to lower the influence of the Galactic MF we accepted only sources with $|b| > 20^\circ$, and we dismissed all the sources with $|\text{RM}| > 300 \text{ rad m}^{-2}$ owing to the fact that RMs obtained in two close frequencies are not fully reliable if their absolute values are too large (Taylor et al. 2009). That left us with 3647 sources.

Removing the GMF. Each observed RM is the sum of several contributions: the one due to the regular GMF which we denote RM_{gal} , the one due to rGMF, the RM intrinsic to the source, and finally the rotation acquired while travelling through the intergalactic medium.

Due to their random character, the last three contributions cannot be separated on a source-by-source basis. On the contrary, RM_{gal} can, in principle, be estimated and subtracted for each source:

$$\text{RRM} = \text{RM} - \text{RM}_{\text{gal}}.$$

where we introduced the residual RM (RRM). Clearly, any redshift evolution or correlation with luminosity would have a more pronounced effect on RRM than on RM.

The Galactic contribution RM_{gal} was estimated using the observed RMs themselves. In order to do so, we first cleaned the *full* NVSS RM catalogue removing the outliers following the algorithm described in (Pshirkov et al. 2013) (a similar approach was used in (Xu & Han 2014), while an alternative algorithm has been devised and applied in (Oppermann et al. 2012, 2014): our results are unchanged if we employ their compilation; notice also that ionospheric RM variation is negligible: (Sotomayor-Beltran et al. A58)). This algorithm is very simple: a circle of 3° radius was circumscribed around every source in the catalogue and both the average RM and its variance were calculated for the selected region. If the RM of the source was more than two r.m.s. values away from the average, the source was marked as “outlier”. In total, 1974 sources were removed after this procedure, leaving 35,569 in the clean set.

Then, for each source with an assigned redshift, we averaged the RMs from the cleaned catalogue within the 3° circle around the source (typically, about 30 values). We interpreted the average as RM_{gal} corresponding to that source. Within the same circle, we also calculated the standard deviation σ_{RM} , which measures the dispersion of RM due to the rGMF and other factors. The contributions to σ_{RM} are assumed to be simple Gaussian errors on each individual source, including measurement errors.

Luminosity. We employed the spectral indices reported in the recent work (Farnes et al. 2014): we first identified as many sources as possible from the (Hammond et al. 2012) set, and assigned them their respective α . We were able to do so for overall 3051 sources out of 3647.

Once the spectral index was assigned to as many sources as possible, we calculated the luminosity with the help of the relation

$$L_{1.4\text{GHz}} = \frac{4\pi D_L^2 S_{1.4\text{GHz}}}{(1+z)^{\alpha+1}}, \quad (3)$$

where D_L is the luminosity distance and $S_{1.4\text{GHz}}$ the flux

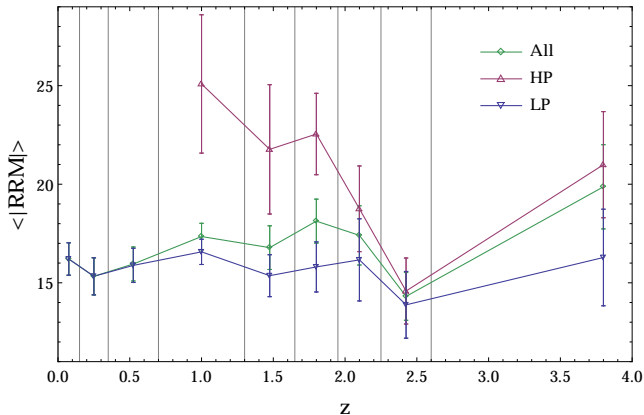


Figure 1. Redshift-dependence of $\langle |RRM| \rangle$ for the entire set, and for the (lp) and (hp) sets separately. All quantities are expressed in rad/m^2 .

density at 1.4 GHz (Hogg 1999). In calculating the luminosity distance D_L we chose a $\Omega_m = 0.73$, $\Omega_\Lambda = 0.27$, and $H = 71 \text{ km/s/Mpc}$.

In the Appendix we show that our results do not change if we employ our own independent compilation of spectral indices.

3 RESULTS

With the final set at hand, we binned all sources in redshift. The criteria with which we chose the bins are explained below. We define the averages $\langle RRM \rangle \equiv \sum_{\text{bin}} RRM/N$, with N the number of sources in each bin, that is, the mean RRM in each (redshift, latitude) bin. We work with the means (rather than, say, variances) because they are believed to be more sensitive to the presence of intergalactic magnetic fields, see (Blasi et al. 1999). Similarly, $\langle \sigma_{RM} \rangle \equiv \sum_{\text{bin}} \sigma_{RM}/N$.

We will use $\langle \sigma_{RM} \rangle$ to estimate the combined contribution of the rGMF, source-intrinsic RM, measurement errors, and the intergalactic magnetic field on the RRM of our target sources. We assume that these contributions to RRM have very similar statistical distributions for nearby lines of sight; in that case the σ_{RM} that we calculate from surrounding sources also measures the spread in RRM that we would expect for each target source if its RRM follows the same distribution as the RRM of surrounding targets.

Notice that here, as well as everywhere else in the paper, the errors are given by $\sigma(|RRM|)_{\text{bin}}/\sqrt{N}$ (and similarly for σ_{RM} : $\sigma(\sigma_{RM})_{\text{bin}}/\sqrt{N}$), where $\sigma(X)$ is the standard deviation of X , and N the number of sources in each bin.

One last note about notation: in all our figures where rotation measures appear, it is intended that their units are always rad/m^2 —we omit these in the figures to avoid cluttering them. Fig. 1 (green diamonds) shows that there might exist an apparent redshift evolution of $\langle |RRM| \rangle$; in fact, our results appear in good qualitative agreement with the results of (Neronov et al. 2013). The quantitative difference could arise due to the different procedures of foreground (i.e., GMF) subtraction.

However, this agreement disappears after we further

z_m	0.075	0.25	0.525	1.0	1.475	1.8	2.1	2.425	3.8
(lp)	418	418	501	677	291	137	76	50	25
(hp)	0	0	5	68	83	72	70	79	80

Table 1. Number of sources in the (lp) and (hp) sets in each redshift bin with mean redshift z_m . Notice that the overall count is 3050 (not 3051), since one source has $z > 5$.

split the set of sources into two subsets according to their intrinsic radio luminosity. Placing the luminosity cut-off at $L = 10^{27.8} \text{ WHz}^{-1}$ gives 2593 sources in the low-power (lp) group, and 457 sources in the high-power (hp) group. This luminosity cut-off allows us to use six bins at high redshift and high radio luminosity. We tried several combinations of redshift bins and luminosity cut-offs, and settled for one which gives us a sufficiently large sample of sources in each bin in Galactic latitude or redshift, as well as enough resolution to check for trends with Galactic latitude or redshift. The limited number of available sources makes it impossible to split the data even further into, for example, sources with different physical properties.

The binning procedure was as follows.

- We first looked at the high power set. Going from the highest z , we chose the bins such that there are about 80 (hp) sources in each bin. This gave us 6 bins starting at redshift $z = 0.7$ and upward.
- At redshifts below 0.7 there are only 5 sources in the (hp) sample. For this reason, at low redshifts the binning was set according to the (lp) sample. We decided to keep three additional low-redshift bins and again chose the bin boundaries so as to have about the same number of events in each bin.

The resulting mean redshifts of the bins z_m —starting from $z = 0$, as well as the numbers of (lp) and (hp) sources in each bin are summarised in Table 1.

The upward and downward triangle points in Fig. 1 show the impact of the separation into the (lp) and (hp) sets. There seems to be a systematic shift in $\langle |RRM| \rangle$ between the two sets; the shift is not very large (on the order of 5 rad m^{-2}) but is coherent throughout most of the bins. At the same time, neither (lp) nor (hp) separately show a systematic dependence of $\langle |RRM| \rangle$ with z .

The most straightforward interpretation of this first result is that: (a) there is no significant evolution with redshift, and (b) higher $\langle |RRM| \rangle$ correlate with higher power.

The featureless binning in z for the (lp) set seems also to be at odds with the model proposed in (Beck et al. 2013). The final result of the galactic dynamics outlined in that work is that it is not uncommon for host galaxies to possess extended and strongly magnetised halos, which result in a (truly) intrinsic RM around 1000 rad m^{-2} already at $2 < z < 4$; if this type of galaxy represented a significant part of our sample then $\langle |RRM| \rangle$ would increase up to 300 rad m^{-2} at these redshifts, the cutoff in rotation measures that we imposed in this work: this is not the case in our analysis.

Motivated by this initial result, we have performed several tests in order to assess the validity of this conclusion. Fig. 2 shows again $\langle |RRM| \rangle$ now together with $\langle \sigma_{RM} \rangle$ for the (lp) and (hp) sets. There is nearly no difference in the $\langle \sigma_{RM} \rangle$

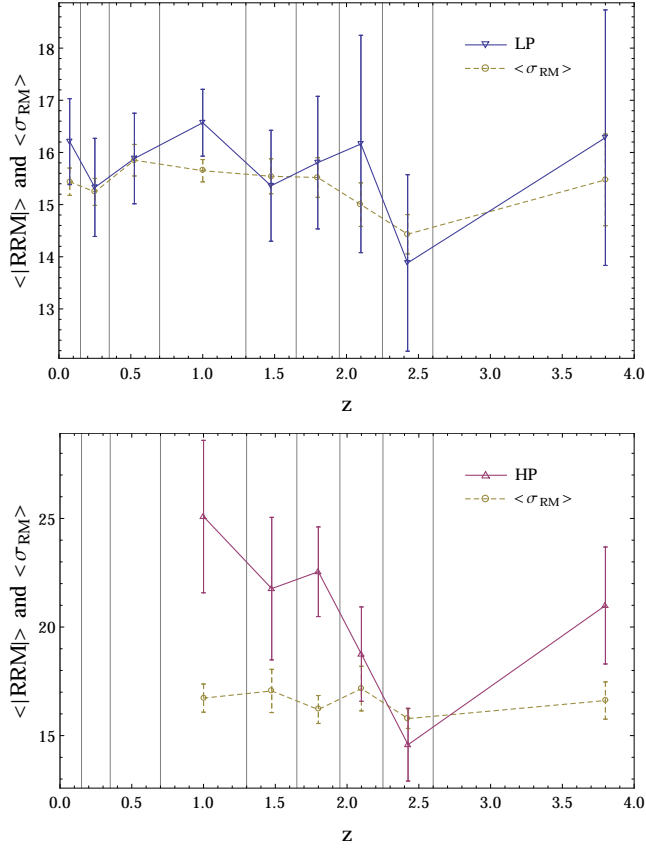


Figure 2. Redshift dependence of $\langle |RRM| \rangle$ and $\langle \sigma_{RM} \rangle$ in the (lp) (upper panel) and (hp) (lower panel) groups. All quantities are expressed in rad/m^2 .

for the two sets, as could be expected because the $\langle \sigma_{RM} \rangle$ are calculated from the full NVSS RM catalogue. Second, there is no obvious trend with redshift for the variances.

In Fig. 3 we have binned the data in Galactic latitude instead of redshift. $\langle \sigma_{RM} \rangle$ shows a very clear dependence on latitude b , which can be modelled by a latitude-dependent component plus a constant value of 13 rad m^{-2} (Pshirkov et al. 2013). This is nicely compatible, numerically as well as qualitatively, with the results of (Schnitzeler 2010), where the latitude dependence of the variance was pointed out, and the different contributions were identified. The $\langle |RRM| \rangle$ of data points in the (lp) category are compatible with $\langle \sigma_{RM} \rangle$, but the $\langle |RRM| \rangle$ of the (hp) ones present a systematic coherent shift over $\langle \sigma_{RM} \rangle$ by about 5 rad m^{-2} .

It is tempting to interpret the absence of redshift evolution in the (lp) group as most likely coming from the turbulent magnetic field of the Milky Way itself, but also errors associated with each RM measurement contribute significantly to the RRM of the (lp) sources.

There is the possibility that the features observed when marginalising over one variable (latitude b or redshift z) could pollute the other “alternative” marginalisation. We did check for this possibility by only choosing higher latitudes, where $\langle \sigma_{RM} \rangle$ is constant, or different redshift bin sizes, and we did not observe any significant departure from the conclusions we arrive at.

In principle a possible explanation for the different be-

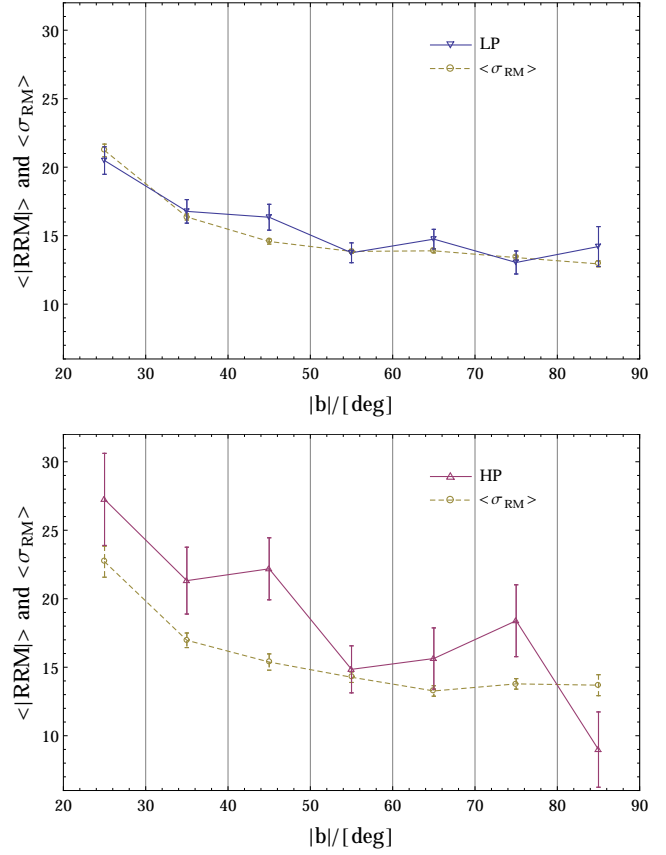


Figure 3. Latitude dependence of $\langle |RRM| \rangle$ and $\langle \sigma_{RM} \rangle$ in the (lp) (upper panel) and (hp) (lower panel) groups. All quantities are expressed in rad/m^2 .

haviour of the (hp) group could be that the sources in this group are distributed differently, i.e. closer to the Galactic plane, and that would lead to the observed excess. In fact, there is a slight preference for low- b in the (hp) set; however, as we demonstrated, it is impossible to attribute all our excess to this small “bias” when we binned with latitude itself. This explanation is therefore ruled out. That means that the positive correlation between the $|RRM|$ and radio luminosity is real, and seemingly compatible with its arising close to the source.

We now turn our attention to the effect of the luminosity cutoff, to check for a possible dependence on the particular value we have chosen. We begin with Fig. 4: we show here the double averaged $|RRM|$ (average over all targets in each latitude bin, then averaged over all latitude bins) of all sources in the (hp) set, as a function of the radio luminosity where we split the entire set in two. The trend towards a more pronounced $|RRM|$ with more severe threshold is very clear. This shows how the threshold itself is not important, and that in fact if we were to choose a cut-off at higher luminosity, were we not limited by statistics, the results would be even more significant. We reach the same conclusion if we only include sources above a certain redshift. Therefore, distance-related selection effects are not important in our analysis.

To include also the change in $\langle \sigma_{RM} \rangle$ as a function of Galactic latitude in our discussion of Fig. 4, we calculate

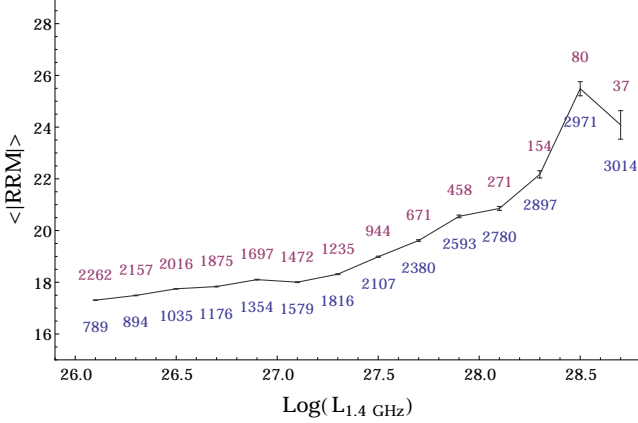


Figure 4. Overall mean $|RRM|$ for the (hp) set plotted against luminosity cut. The values above and below the curve are the number of events at given power threshold in the (hp) and (lp) sets, respectively, as defined by the cut. All quantities are expressed in rad/m^2 .

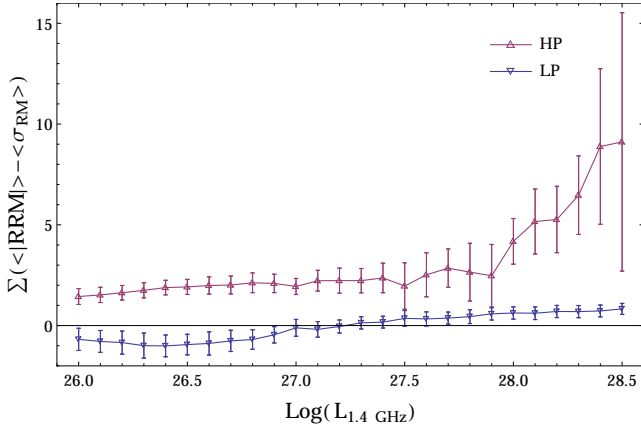


Figure 5. Sum of the differences $\langle |RRM| \rangle - \langle \sigma_{RM} \rangle$ for the (lp) and (hp) sets in each latitude bin, followed by summing all latitude bins, plotted against the power cutoff threshold. All quantities are expressed in rad/m^2 .

the difference between $\langle |RRM| \rangle$ and $\langle \sigma_{RM} \rangle$ for each latitude bin from Fig. 3, then sum all latitude bins. This was done for varying luminosity cutoffs, similarly to Fig. 4. The results are presented in Fig. 5. Independent of our choice for the luminosity cut-off, the $\langle |RRM| \rangle$ of sources from the (lp) set are consistent with $\langle \sigma_{RM} \rangle$. On the other hand, the $\langle |RRM| \rangle$ of sources from the (hp) set are incompatible with $\langle \sigma_{RM} \rangle$ for all luminosity cut-offs. This strengthens the conclusion that we reached from analysing Fig. 3, which was limited to a single luminosity cut-off. Bear in mind that only the difference in behaviour between the (lp) and (hp) sources matters here, not the actual values of $\langle |RRM| \rangle - \langle \sigma_{RM} \rangle$ (which in fact are not predictable individually).

Having established that there seems to be a positive correlation between RRM and luminosity, a legitimate question is whether a relatively small group of sources with (perhaps) extreme properties is driving this result—for instance, there could be different populations of sources with different intrinsic properties. Removing sources from the (hp) set with

large $|RRM|$ still produces an offset, but the error bars increase, and it is no longer clear if these $\langle |RRM| \rangle$ are incompatible with $\langle \sigma_{RM} \rangle$ in this case. Also, employing the spectral index α as discriminant, we were not able to clearly discern between two (or more) populations, and we did not observe any particular trend of the spectral index α with RRM itself.

Yet another possibility, put forward in the works of (Joshi & Chand 2013; Farnes et al. 2014; Banfield et al. 2014), is that the effect could be caused not by intervening filaments but by smaller systems like MgII absorbers. Thence, sources with MgII absorption along the line of sight have higher RMs than those without absorption. Since sources at higher redshifts (and hence preferentially higher luminosities) have more absorbers than sources at low redshifts (where although high luminosities are present, on average their luminosities will be lower), the correlation we observe might be a result of the intervening systems rather than due to luminosity itself. If this were true, however, we would see this in both (lp) and (hp) sets, but the former does not show any such effect (although the fluctuations due to measurement errors and the random GMF can be large).

4 SUMMARY

To conclude, we briefly recapitulate the salient features of our searches. We set out with the purpose of investigating the possibility of a redshift dependence in the observed Faraday sky, investigation which we based on the set of all NVSS catalogue sources for which redshift information is known—this is the largest available set in the literature at the moment. The catalogue was cleaned removing outliers with potentially unreliable RMs; we then used the data itself to separate the RM due to the regular MF of the Milky Way: all our statistical results are based on the *residual* RM ($|RRM|$).

We specifically looked for the effect of the radio luminosity $L_{1.4\text{GHz}}$ of the sources (calculated independently for most sources through their flux densities); this effect and our interpretation of our results can be summarised in these seven points below.

- The $|RRM|$ positively correlates with $L_{1.4\text{GHz}}$, that is, the higher luminosity sources have higher residual RMs (Fig. 4).
- The $|RRM|$ of low luminosity sources is dominated by the variance due to measurement errors and that coming from the rGMF (Figs. 2 and 3, top). The overall $|RRM|$ consistently decreases with latitude as we move away from the Galactic plane.
- The $|RRM|$ of high power sources, on the other hand, stands out coherently above the expected σ_{RM} variance; this is true in both redshift and latitude bins, where in the latter it is also easy to single out the Galactic contribution (Figs. 2 and 3, bottom).
- Therefore, there is an *overall* shift in $|RRM|$ between the two sets. This shift appears in redshift bins (Figs. 1 and 2) as well as in latitude bins (again Fig. 3), and amounts to the same value of approximately 5 rad m^{-2} for a split at $\log L_{1.4\text{GHz}} = 27.8$.
- The systematic shift is not an artifact of the luminosity cutoff, as it actually grows with more constraining choices (Figs. 4 and 5).

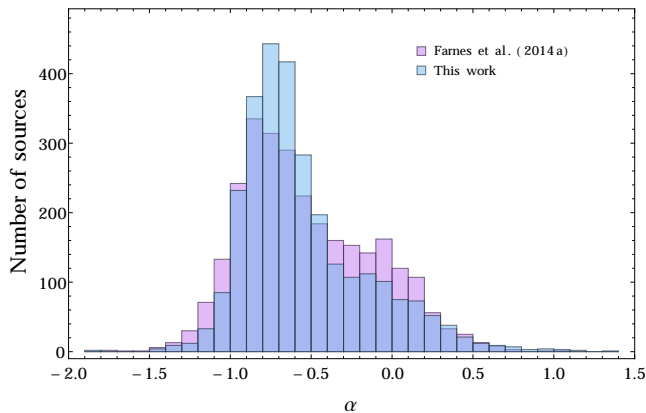


Figure 6. The different α distributions for the common 2830 sources of (Farnes et al. 2014) and those identified with our own compilation of VLSS, WENSS, SUMSS, and VeV.

- The systematic shift is also not an artifact of redshift evolution, as we do not observe any trend in the z behaviour of either set (Figs. 1 and 2).

- If we ignore the luminosity and analyse the full catalogue we do observe a weak redshift dependence (Fig. 1), which we can hence impute to a Malmquist bias, i.e., from larger distances brighter sources are more easily detected. Again, what does appear to correlate are $|\text{RRM}|$ and luminosity, not redshift.

These results are promising, and it would be extremely useful to understand if this correlation is physical and isolate its origin: we performed a few tests in this sense but the statistical size of the sample was too limiting a factor. In particular it would be very interesting to see whether the correlation and/or the systematic shift are driven by a particular set of sources, for instance a small set belonging to a particular type of objects. With a larger dataset these questions could be easily addressed; a larger set would also allow a much better estimation of the Galactic contribution, and would finally shed light on possible features as for any redshift development of $|\text{RRM}|$. We leave all these updates for future investigations.

ACKNOWLEDGEMENTS

The authors would like to thank B Gaensler and J L Han for positive feedback and useful correspondence. MP wishes to thank the Service de Physique Théorique in Brussels, where this work was conceived. The work of MP is supported by RFBR Grants No. 13-02-01293a, by the Grant of the President of Russian Federation MK-2138.2013.2 and by the Dynasty Foundation. FU and PT are supported by IISN project No. 4.4502.13 and Belgian Science Policy under IAP VII/37. PT is supported in part by the RFBR grant 13-02-12175-ofm. This research has made use of NASA’s Astrophysics Data System.

z_m	0.075	0.25	0.525	1.0	1.475	1.8	2.1	2.425	3.8
(<i>lp</i>)	474	450	528	693	289	135	74	51	27
(<i>hp</i>)	0	0	5	74	81	76	77	78	78

Table 2. Number of sources in the (*lp*) and (*hp*) sets in each redshift bin for our set of sources with manually calculated luminosity. The overall count is of 3190 objects.

APPENDIX

One crucial ingredient in this analysis is the intrinsic luminosity of the sources. In addition to using the compilation of (Farnes et al. 2014), we have manually computed the spectral indices of as many sources as possible using information from three additional catalogues: VLSS² (74 MHz, $\text{dec} > -30^\circ$), WENSS³ (352 MHz, $\text{dec} > 28.5^\circ$), and SUMSS⁴ (843 MHz, $\text{dec} < -30^\circ$), from which we can calculate the spectral index α of the source. When combined, they nicely cover all the sky. The algorithm to obtain the intrinsic power of each source was as follows:

- for each item in the catalogue of (Hammond et al. 2012) (with additional cuts at $|b| > 20^\circ$ and $|\text{RM}| < 300 \text{ rad m}^{-2}$) we found the counterpart in one or more of the three catalogues mentioned above;
- wherever possible, that is, where at least two different fluxes are available, we calculated α ;
- if α could be calculated from either SUMSS or WENSS we employed these values, because all VLSS entries have larger error;
- conversely, if only data from VLSS was available, we used the latter;
- only as a last option we calculated α from the (Véron-Cetty & Véron 2010) compilation as it is comparatively less reliable.

With this procedure, we obtained the final set of 3190 sources (out of the original 3647) for which α was assigned, while with (Farnes et al. 2014) we were able to work with 3050 sources. In Fig. 6 we show the different distributions for the sources which belong to both catalogues.

After calculating the luminosities again using Eq. 3 we can perform the analysis as we did in the main text. We report here only the most relevant plots, that is, Fig. 7 with the redshift-binned $|\text{RRM}|$ for the split set, (analogue to Fig. 1), and Fig. 8 showing the luminosity-RM correlation (analogue to Fig. 4).

The features which we observed in the main text appear here unchanged—in fact, they are even more prominent: there is a positive correlation between the observed residual RM and the luminosity.

² VLA Low-Frequency Sky Survey (Cohen et al. 2007).

³ The Westerbork Northern Sky Survey (Rengelink et al. 1997) <http://www.astron.nl/wow/testcode.php?survey=1&more=1>.

⁴ The Sydney University Molonglo Sky Survey (Bock et al. 1999; Mauch et al. 2003).

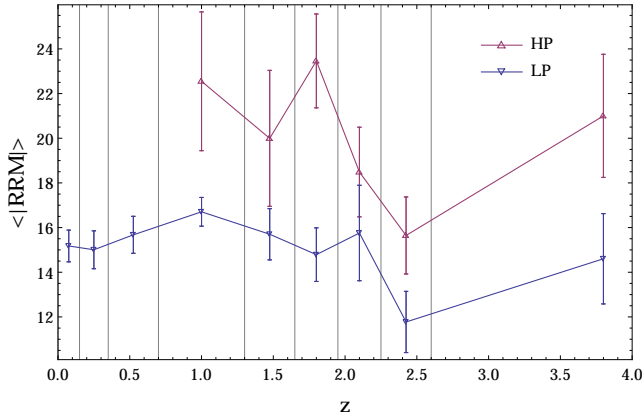


Figure 7. Mean $\langle |RRM| \rangle$ in z -bins for (lp) and (hp) sets separately for our set of sources with manually calculated luminosity. All quantities are expressed in rad/m^2 .

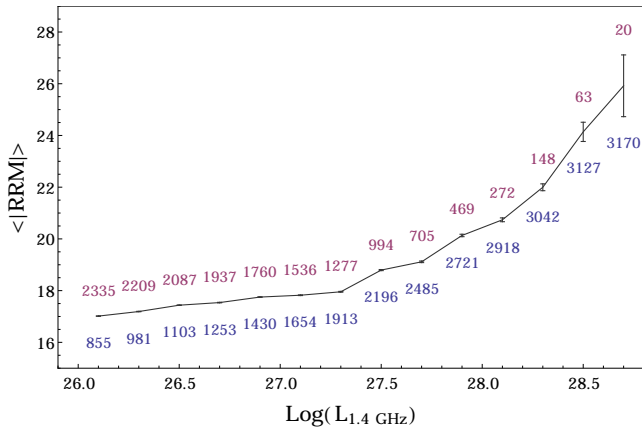


Figure 8. Overall mean $|RRM|$ for the (hp) set plotted against luminosity cut. The values above and below the curve are the number of events at given power threshold in the (hp) and (lp) sets, respectively, as defined by the cut. All quantities are expressed in rad/m^2 .

REFERENCES

- Banfield J. K., Schnitzeler D. H. F. M., George S. J., Norris R. P., Jarrett T. H., Taylor A. R., Stil J. M., 2014, arXiv:1404.1638 [astro-ph.GA]
- Beck A. M., Dolag K., Lesch H., Kronberg P. P., 2013, MNRAS, 435, 3575
- Beck A. M., Hanasz M., Lesch H., Remus R.-S., Stasyszyn F. A., 2013, MNRAS, 429, L60
- Bernet M. L., Miniati F., Lilly S. J., Kronberg P. P., Dessauges-Zavadsky M., 2008, Nature, 454, 302
- Blasi P., Burles S., Olinto A. V., 1999, Astrophys.J., 514, L79
- Bock D. C.-J., Large M. I., Sadler E. M., 1999, AJ, 117, 1578
- Broderick A. E., Chang P., Pfrommer C., 2012, Astrophys.J., 752, 22
- Cohen A. S., Lane W. M., Cotton W. D., Kassim N. E., Lazio T. J. W., Perley R. A., Condon J. J., Erickson W. C., 2007, AJ, 134, 1245
- Condon J. J., Cotton W., Greisen E., Yin Q., Perley R., et al., 1998, Astron.J., 115, 1693
- Dolag K., Kachelriess M., Ostapchenko S., Tomas R., 2011, Astrophys.J., 727, L4
- Dolgov A. D., 2003, arXiv:astro-ph/0306443
- Durrer R., Neronov A., 2013, Astron.Astrophys.Rev., 21, 62
- Farnes J., Gaensler B., Carretti E., 2014, Astrophys.J.Suppl., 212, 15
- Farnes J., O'Sullivan S., Corrigan M., Gaensler B., 2014
- Govoni F., Feretti L., 2004, Int.J.Mod.Phys., D13, 1549
- Grasso D., Rubinstein H. R., 2001, Phys.Rept., 348, 163
- Hammond A. M., Robishaw T., Gaensler B. M., 2012, arXiv:1209.1438 [astro-ph.CO]
- Han J.-L., Wielebinski R., 2002, Chin.J.Astron.Astrophys., 2, 293
- Hogg D. W., 1999, arXiv:astro-ph/9905116
- Joshi R., Chand H., 2013, Mon.Not.Roy.Astron.Soc., 434, 3566
- Kandus A., Kunze K. E., Tsagas C. G., 2011, Phys.Rept., 505, 1
- Kronberg P., Bernet M., Miniati F., Lilly S., Short M., et al., 2008, Astrophys.J., 676, 7079
- Kronberg P. P., 1994, Rept.Prog.Phys., 57, 325
- Mauch T., Murphy T., Buttery H. J., Curran J., Hunstead R. W., Piestrzynski B., Robertson J. G., Sadler E. M., 2003, MNRAS, 342, 1117
- Miniati F., Elyiv A., 2013, Astrophys.J., 770, 54
- Murase K., Dermer C. D., Takami H., Migliori G., 2012, Astrophys.J., 749, 63
- Neronov A., Semikoz D., Banafsheh M., 2013, arXiv:1305.1450 [astro-ph.CO]
- Neronov A., Taylor A., Tchernin C., Vovk I., 2013, Published in A&A, p. 554
- Neronov A., Vovk I., 2010, Science, 328, 73
- Oppermann N., Junklewitz H., Greiner M., Enßlin T. A., Akahori T., et al., 2014
- Oppermann N., Junklewitz H., Robbers G., Bell M., Enßlin T., et al., 2012, Astron.Astrophys., 542, A93
- Pshirkov M. S., Tinyakov P. G., Urban F. R., 2013, MNRAS, 436, 2326
- Rengelink R. B., Tang Y., de Bruyn A. G., Miley G. K., Bremer M. N., Roettgering H. J. A., Bremer M. A. R., 1997, A&AS, 124, 259
- Ryu D., Schleicher D. R. G., Treumann R. A., Tsagas C. G., Widrow L. M., 2012, Space Sci. Rev., 166, 1
- Saveliev A., Evoli C., Sigl G., 2013, arXiv:1311.6752 [astro-ph.HE]
- Schnitzeler D., 2010, Mon.Not.Roy.Astron.Soc., 409, L97
- Sironi L., Giannios D., 2014, Astrophys.J., 787, 49
- Sotomayor-Beltran C., Sobey C., Hessels J., de Bruyn G., Noutsos A., et al., A58, Astron.&Astrophys. 552, p. 2013
- Tavecchio F., Ghisellini G., Foschini L., Bonnoli G., Ghirlanda G., et al., 2010, Mon.Not.Roy.Astron.Soc., 406, L70
- Taylor A., Stil J., Sunstrum C., 2009, Astrophys.J., 702, 1230
- Taylor A., Vovk I., Neronov A., 2011, Astron.Astrophys., 529, A144
- Vallée J. P., 2004, New Astron.Rev., 48, 763
- Véron-Cetty M.-P., Véron P., 2010, A&A, 518, A10
- Xu J., Han J. L., 2014, arXiv:1405.5087 [astro-ph.CO]